

Controllable broadband nonlinear optical response of graphene dispersions by tuning vacuum pressure

Xin Cheng,¹ Ningning Dong,^{1,5} Bin Li,² Xiaoyan Zhang,¹ Saifeng Zhang,¹ Jia Jiao,³
Werner J. Blau,^{1,4} Long Zhang,¹ and Jun Wang^{1,*}

¹Key Laboratory of Materials for High Power Laser, Shanghai Institute of Optics and fine Mechanics, Chinese Academy of Sciences, Shanghai 201800, China

²Military Representative Bureau in Xi'an, Xi'an, Shaanxi Province 710000, China

³Research Laboratory for High Density Optical Storage, Shanghai Institute of Optics and fine Mechanics, Chinese Academy of Sciences, Shanghai 201800, China

⁴School of Physics and the Centre for Research on Adaptive Nanostructures and Nanodevices (CRANN), Trinity College Dublin, Dublin 2, Ireland

⁵n.n.dong@siom.ac.cn

*jwang@siom.ac.cn

Abstract: Nonlinear scattering, originating from laser induced solvent micro-bubbles and/or micro-plasmas, is regarded as the principal mechanism for nonlinear optical (NLO) response of graphene dispersions at ns timescale. In this work, we report the significant enhancement of NLO response of graphene dispersions by decreasing the atmospheric pressure, which has strong influence on the formation and growth of micro-bubbles and/or micro-plasmas. A modified open-aperture Z-scan apparatus in combination with a vacuum system was used to study the effect of vacuum pressure on the NLO property of graphene dispersions prepared by liquid-phase exfoliation technique. We show that the atmospheric pressure can be utilized to control and tune the nonlinear responses of the graphene dispersions for ns laser pulses at both 532 nm and 1064 nm. The lower the vacuum pressure was, the larger the NLO response was. In contrast, the NLO property of fullerene was found to be independent of the pressure change, due to its nature of nonlinear absorption. This work affords a simple method to distinguish the nonlinear scattering and absorption mechanisms for NLO nanomaterials.

©2013 Optical Society of America

OCIS codes: (140.3538) Lasers, pulsed; (160.4330) Nonlinear optical materials; (290.4020) Mie theory.

References and links

1. K. S. Novoselov, A. K. Geim, S. V. Morozov, D. Jiang, Y. Zhang, S. V. Dubonos, I. V. Grigorieva, and A. A. Firsov, "Electric field effect in atomically thin carbon films," *Science* **306**(5696), 666–669 (2004).
2. A. K. Geim and K. S. Novoselov, "The rise of graphene," *Nat. Mater.* **6**(3), 183–191 (2007).
3. S. V. Morozov, K. S. Novoselov, M. I. Katsnelson, F. Schedin, D. C. Elias, J. A. Jaszczak, and A. K. Geim, "Giant intrinsic carrier mobilities in graphene and its bilayer," *Phys. Rev. Lett.* **100**(1), 016602 (2008).
4. K. I. Bolotin, K. J. Sikes, Z. Jiang, M. Klima, G. Fudenberg, J. Hone, P. Kim, and H. L. Stormer, "Ultrahigh electron mobility in suspended graphene," *Solid State Commun.* **146**(9–10), 351–355 (2008).
5. K. S. Kim, Y. Zhao, H. Jang, S. Y. Lee, J. M. Kim, K. S. Kim, J. H. Ahn, P. Kim, J. Y. Choi, and B. H. Hong, "Large-scale pattern growth of graphene films for stretchable transparent electrodes," *Nature* **457**(7230), 706–710 (2009).
6. R. R. Nair, P. Blake, A. N. Grigorenko, K. S. Novoselov, T. J. Booth, T. Stauber, N. M. R. Peres, and A. K. Geim, "Fine structure constant defines visual transparency of graphene," *Science* **320**(5881), 1308 (2008).
7. A. A. Balandin, S. Ghosh, W. Z. Bao, I. Calizo, D. Teweldebrhan, F. Miao, and C. N. Lau, "Superior thermal conductivity of single-layer graphene," *Nano Lett.* **8**(3), 902–907 (2008).
8. D. R. Dreyer, S. Park, C. W. Bielawski, and R. S. Ruoff, "The chemistry of graphene oxide," *Chem. Soc. Rev.* **39**(1), 228–240 (2009).
9. F. Bonaccorso, Z. Sun, T. Hasan, and A. C. Ferrari, "Graphene photonics and optoelectronics," *Nat. Photonics* **4**(9), 611–622 (2010).

10. K. P. Loh, Q. L. Bao, G. Eda, and M. Chhowalla, "Graphene oxide as a chemically tunable platform for optical applications," *Nat. Chem.* **2**(12), 1015–1024 (2010).
11. J. Wang, Y. Hernandez, M. Lotya, J. N. Coleman, and W. J. Blau, "Broadband nonlinear optical response of graphene dispersions," *Adv. Mater.* **21**(23), 2430–2435 (2009).
12. J. Wang and W. J. Blau, "Inorganic and hybrid nanostructures for optical limiting," *J. Opt. A* **11**(2), 024001 (2009).
13. Y. Chen, Y. Lin, Y. Liu, J. Doyle, N. He, X. D. Zhuang, J. R. Bai, and W. J. Blau, "Carbon nanotube-based functional materials for optical limiting," *J. Nanosci. Nanotechnol.* **7**(4-5), 1268–1283 (2007).
14. G. Bottari, G. de la Torre, D. M. Guldi, and T. Torres, "Covalent and noncovalent phthalocyanine-carbon nanostructure systems: synthesis, photoinduced electron transfer, and application to molecular photovoltaics," *Chem. Rev.* **110**(11), 6768–6816 (2010).
15. J. Wang, Y. Chen, and W. J. Blau, "Carbon nanotubes and nanotube composites for nonlinear optical devices," *J. Mater. Chem.* **19**(40), 7425–7443 (2009).
16. J. Wang, D. Früchtl, Z. Y. Sun, J. N. Coleman, and W. J. Blau, "Control of optical limiting of carbon nanotube dispersions by changing solvent parameters," *J. Phys. Chem. C* **114**(13), 6148–6156 (2010).
17. J. Wang, D. Früchtl, and W. J. Blau, "The importance of solvent properties for optical limiting of carbon nanotube dispersions," *Opt. Commun.* **283**(3), 464–468 (2010).
18. Y. Hernandez, V. Nicolosi, M. Lotya, F. M. Blighe, Z. Sun, S. De, I. T. McGovern, B. Holland, M. Byrne, Y. K. Gun'ko, J. J. Boland, P. Niraj, G. Duesberg, S. Krishnamurthy, R. Goodhue, J. Hutchison, V. Scardaci, A. C. Ferrari, and J. N. Coleman, "High-yield production of graphene by liquid-phase exfoliation of graphite," *Nat. Nanotechnol.* **3**(9), 563–568 (2008).
19. S. D. Bergin, V. Nicolosi, P. V. Streich, S. Giordani, Z. Y. Sun, A. H. Windle, P. Ryan, N. P. Niraj, Z. T. Wang, L. Carpenter, W. J. Blau, J. Boland, J. P. Hamilton, and J. N. Coleman, "Towards solutions of single-walled carbon nanotubes in common solvents," *Adv. Mater.* **20**(10), 1876–1881 (2008).
20. J. Wang and W. J. Blau, "Solvent effect on optical limiting properties of single-walled carbon nanotube dispersions," *J. Phys. Chem. C* **112**(7), 2298–2303 (2008).
21. J. Wang and W. J. Blau, "Nonlinear optical and optical limiting properties of individual single-walled carbon nanotubes," *Appl. Phys. B* **91**(3–4), 521–524 (2008).
22. L. W. Tutt and T. F. Boggess, "A review of optical limiting mechanisms and devices using organics, fullerenes, semiconductors and other materials," *Prog. Quantum Electron.* **17**(4), 299–338 (1993).
23. J. Wang and W. J. Blau, "Linear and nonlinear spectroscopic studies of phthalocyanine-carbon nanotube blends," *Chem. Phys. Lett.* **465**(4–6), 265–271 (2008).
24. J. H. Zhu, Y. X. Li, Y. Chen, J. Wang, B. Zhang, J. J. Zhang, and W. J. Blau, "Graphene oxide covalently functionalized with zinc phthalocyanine for broadband optical limiting," *Carbon* **49**(6), 1900–1905 (2011).
25. Y. P. Sun and J. E. Riggs, "Organic and inorganic optical limiting materials. From fullerenes to nanoparticles," *Int. Rev. Phys. Chem.* **18**(1), 43–90 (1999).
26. J. J. Doyle, V. Nicolosi, S. M. O'Flaherty, D. Vengust, A. Drury, D. Mihailovic, J. N. Coleman, and W. J. Blau, "Nonlinear optical response of Mo₆S₄S_{4.5} nanowires," *Chem. Phys. Lett.* **435**(1–3), 109–113 (2007).
27. N. Venkatram, D. N. Rao, and M. A. Akundi, "Nonlinear absorption, scattering and optical limiting studies of CdS nanoparticles," *Opt. Express* **13**(3), 867–872 (2005).
28. S. M. O'Flaherty, S. V. Hold, M. J. Cook, T. Torres, Y. Chen, M. Hanack, and W. J. Blau, "Molecular engineering of peripherally and axially modified phthalocyanines for optical limiting and nonlinear optics," *Adv. Mater.* **15**(1), 19–32 (2003).
29. I. M. Belousova, N. G. Mironova, and M. S. Yur'ev, "Theoretical investigation of nonlinear limiting of laser radiation power by suspensions of carbon particles," *Opt. Spectrosc.* **94**(1), 86–91 (2003).
30. G. S. He, H. Y. Qin, and Q. D. Zheng, "Rayleigh, mie, and tyndall scatterings of polystyrene microspheres in water: wavelength, size, and angle dependences," *J. Appl. Phys.* **105**(2), 023110 (2009).

1. Introduction

Graphene has recently attracted enormous attention as a promising candidate material for photonic and optoelectronic devices owing to its unique properties, such as, high carrier mobility, strict optical transparency of single layer, high thermal conductivity, high chemical stability, ultrafast carrier dynamics, etc [1–11]. In addition, the advantage of tailoring properties by attaching functional materials, e.g., polymers, organic molecules and metal nanoparticles, forming versatile graphene composites [12–15], makes graphene play an increasing important role in photonic applications. In our previous works, we reported the NLO properties of a range of functionalized graphene and carbon nanotube composites and developed a series of techniques to improve the NLO response and optical limiting performance of carbon nanostructures [11, 15]. It was found that modifying solvent and increasing temperature can enhance the NLO responses of graphene and carbon nanotube dispersions, in which nonlinear scattering (NLS), originating from laser induced solvent micro-bubbles and/or micro-plasmas, dominates the nonlinear responses [16, 17]. In this work, we investigated the NLO property of liquid-phase exfoliated graphene dispersions, and

provide a simple method to control the nonlinear responses by tuning the vacuum pressure, by which one can affect effectively the size of the scattering centers, i.e., the induced micro-bubbles and micro-plasmas.

2. Experiments

According to the previous experimental and theoretical analyses, the surface energies of N-methyl-2-pyrrolidone (NMP), N,N-dimethyl-formamide (DMF) and sodium cholate (SC) match very well with that of graphite ($70 \sim 80 \text{ mJ/m}^2$), resulting in effective exfoliation to graphene with single or few layers [18, 19]. In this work, high quality graphene dispersions in NMP, DMF and SC were employed for NLO study. The preparation procedure is similar to our previous works [11, 18]. Initial graphite dispersions of 5.0 mg/mL were sonicated for 24 h using a low-power ultrasonic bath (200 W), followed by 24 h standing at room temperature. All these dispersions were subsequently centrifuged at 1500 rpm for 90 min to separate any large aggregates. High quality graphene dispersions were obtained by collecting the top 1/3 part of the centrifuged samples. The dispersions were stable against sedimentation over several weeks. For comparison, fullerene solutions in toluene were prepared by sonicating for 15 min using low-power ultrasonic bath. According to our previous work [11], the size of the graphene nano-flakes is $\sim 0.5\text{-}2 \text{ }\mu\text{m}$ and the number fraction of monolayer graphene (number of monolayers/total number of flakes) in each dispersion is close to 30%.

A modified open-aperture Z-scan apparatus, illustrated in Fig. 1, was used to investigate the NLO property of the graphene dispersions under different vacuum pressures. The optical arrangement was similar to that used in our previous works of testing nonlinear responses of nanotube dispersions [20, 21]. A vacuum system was introduced into the Z-scan setup to tune the pressure in the vacuum chamber where the dispersion samples were placed. The total transmittance through the samples as a function of incident power density was measured while the samples were gradually moved through the focus of a lens along the z-axis. All experiments were performed by using 6 ns pulses from a Q-switched Nd:YAG laser at 1064 nm and its second harmonic of 532 nm with the repetition rate of 2 Hz. The laser beam was tightly focused through a lens with the focal length of 15 cm. All dispersions were tested in $10 \times 10 \text{ mm}$ quartz cuvettes at a linear transmittance of $\sim 50\%$. The beam waist radii of the focus at 532 nm and 1064 nm were estimated to be $\sim 33 \text{ }\mu\text{m}$ and $\sim 61 \text{ }\mu\text{m}$, respectively.

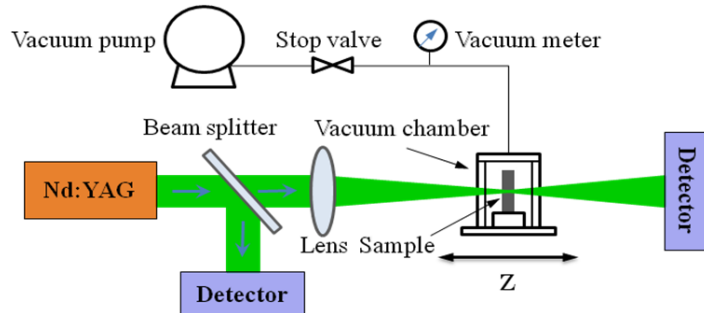


Fig. 1. Schematic of the modified open-aperture Z-scan.

3. Results and discussion

Figures 2(a)-2(b) show the open aperture Z-scan results for the graphene dispersions in NMP at different vacuum pressures. It was observed that the normalized transmission reduced significantly with the decrease of the vacuum pressure for both 532 and 1064 nm pulses. The lower the pressure was, the higher the NLO response was. As shown in Fig. 2, all open-aperture Z-scans performed in this study exhibited a reduction in the transmission about the focus of the lens, implying an effective optical limiting property of the graphene dispersions. Optical limiting is an important NLO phenomenon, which can be utilized to protect delicate optical instruments, especially the human eyes, from intense laser beams [22]. Ideally, an

optical limiter should strongly attenuate intense, potentially dangerous laser beams, while exhibiting high transmittance for low intensity ambient light.

Figure 1(c) shows the Z-scan results for fullerene solutions at different vacuum pressures. In contrast to the graphene dispersions, which exhibit remarkable vacuum dependence effect, the fullerene solutions show NLO response independent of the variation of pressure. For the graphene dispersions, the NLO response is attributed to thermally induced NLS, and the size of the scattering centers, i.e., micro-bubbles and micro-plasmas, varies with the pressure changing. On the contrary, for fullerene, the NLO response is originated from reverse saturable absorption (RSA), which is independent of vacuum [22]. It should be pointed out that this apparatus can be used to distinguish different NLO mechanisms (viz., nonlinear scattering and nonlinear absorption) by changing pressure, hence control the NLS in the hybrid nanocomposites, such as phthalocyanine functionalized carbon nanostructures [23, 24].

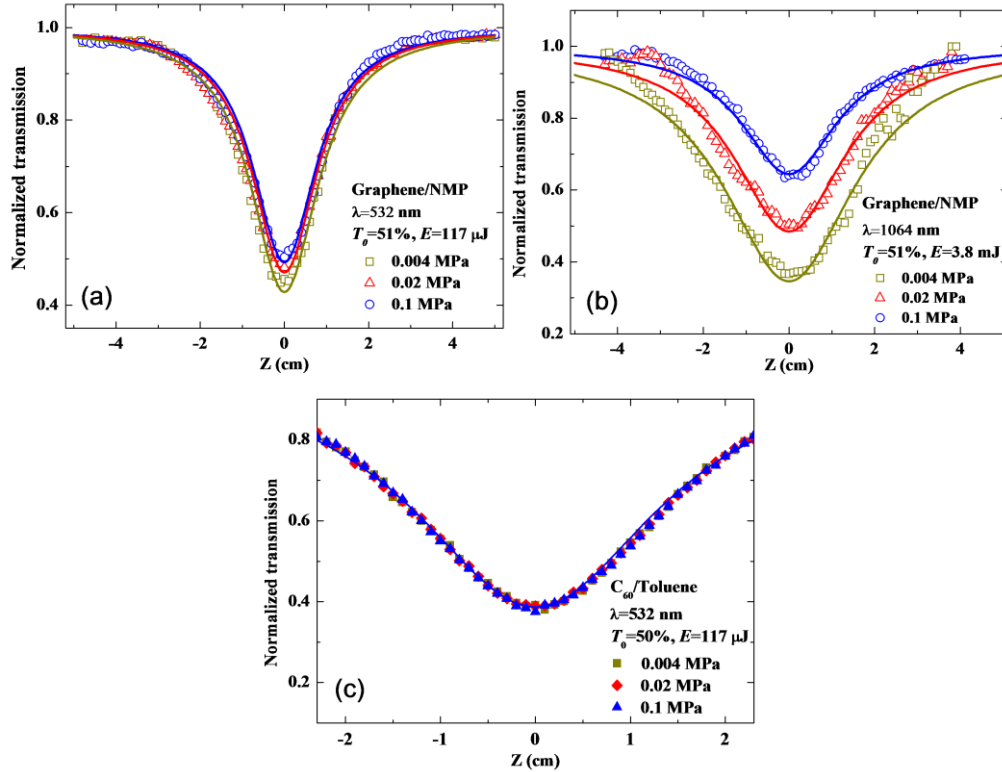


Fig. 2. Typical open-aperture Z-scan data with normalized transmission as a function of the sample position Z for the graphene dispersions in NMP at (a) 532 nm and (b) 1064 nm, and (c) fullerene solutions at 532 nm under different pressures.

Z-scan measurements for the SC and DMF dispersions were also carried out at 532 nm. As shown in Fig. 3, similar to the NMP dispersions, the normalized transmission of both SC and DMF dispersions reduces gradually with the vacuum pressure decreased. These results indicate that NLS dominates the NLO responses of graphene in all the solvents used in this work. We expect the vacuum pressure controlling technique fits not only the graphene dispersions but also other NLS dominated nonlinear nanomaterials [12].

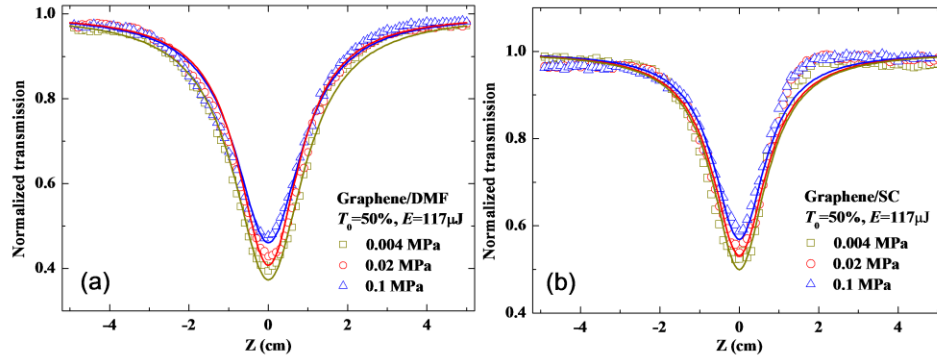


Fig. 3. Typical open-aperture Z-scans for the DMF dispersions (a) and SC dispersions (b) at different atmospheric pressures.

Thermally induced NLS is one common and principal factor for the NLO and optical limiting responses of a range of nanomaterials, such as metal nanoparticles [12, 25], nanowires [26], quantum dots [27], etc. Based on the Mie scattering theory, the effective scattering occurs when the scattering centers, which can be formed by the generation of solvent bubbles and/or the ionization of nanoparticles, reach comparable size to the wavelength of the incident laser beam. In other words, the scattering efficiency is largely dependent on the scattering cross section, hence the size of scattering centers. It has been demonstrated that the size of the scattering centers is determined by a number of factors, such as pulse energy, pulse duration, temperature, and thermo-dynamical/cohesive properties of solvents, etc [12, 15–17, 20, 28]. Here, we show that the size of the scattering centers can also be influenced by the atmospheric pressure. In the assumption of equilibrium condition, the relationship between the bubble size r_B and the atmospheric pressure p_∞ can be estimated through the equation [11]

$$2\gamma = \frac{3nRT}{4\pi r_B^2} - p_\infty r_B \quad (1)$$

where γ is the surface tension, n is the number of moles of gas, R is the universal gas constant, and T is the absolute temperature in the bubbles. In general, the lower the atmospheric pressure p_∞ is, the more quickly the initial micro-bubbles would expand due to the larger pressure difference at the vapor-solution interface, resulting in efficient scattering to the incident beam, and hence more reduction of transmission. Thus, it is reasonable that the nonlinear response of the graphene dispersions can be adjusted by tuning the atmospheric pressure. On the other hand, the RSA induced optical limiting of fullerene is mainly determined by the ability of absorbing photons at 532 nm via its singlet and triplet excited states, thus the pressure would not take effect. This explains why the vacuum pressure can greatly influence the optical limiting performance of the graphene dispersions but have no effect to the fullerene solutions.

In order to have a further understanding on the effect of vacuum pressure, we investigated the nonlinear responses of the graphene dispersions at different input energy densities and solvents at a vacuum pressure of ~ 0.004 MPa. Figure 4(a) manifests the nonlinear response of the NMP dispersions at a series of incident energies. It is evident that for the NMP dispersions, the NLO responses are dramatically improved by increasing the incident energy. Figure 4(b) depicts the comparison of Z-scan curves for the NMP, DMF and SC dispersions. It is clear that the optical limiting performance of the DMF dispersions outperforms those of NMP and SC dispersions. The SC dispersions exhibit an inferior optical limiting effect in comparison with the DMF and NMP dispersions. These results are in accordance with our

previous conclusion that a smaller solvent surface tension results in a higher scattering efficiency and optical limiting ability [11, 20].

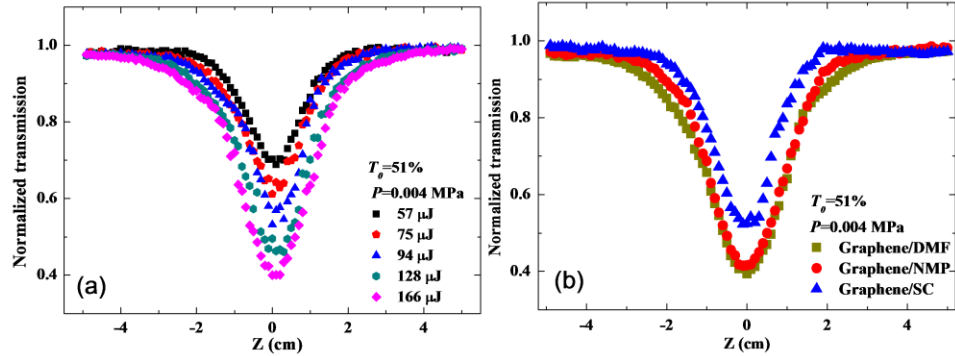


Fig. 4. Typical open-aperture Z-scan at different incident pulse energies (a) and for the three different dispersions (b).

The nonlinear extinction coefficient β_{eff} can be estimated by fitting the Z-scan results [21, 22, 28]. Figure 5(a) shows the vacuum pressure dependent nonlinear extinction coefficient in different dispersions at 532 nm. It is clearly seen that β_{eff} increases gradually with the vacuum pressure decreasing. Furthermore, the DMF dispersions exhibited larger β_{eff} value than the others at the same pressure, and the smallest β_{eff} was observed for the SC dispersions. For example, β_{eff} is 2.89 ± 0.15 , 2.6 ± 0.13 and 2.05 ± 0.10 cm/GW for the DMF, NMP and SC dispersions at the pressure of 0.004 MPa, respectively. The errors in Fig. 5 were calculated from the multiple Z-scan measurements at the same atmospheric pressure. Compared with graphene, β_{eff} for fullerene keeps constant at different vacuum pressures, which is in agreement with the Z-scan results in Fig. 2(c). In addition, we investigated the variation of β_{eff} of the NMP dispersions under different pressures at 532 and 1064 nm. As shown in Fig. 5(b), β_{eff} increases with the decrease of vacuum pressure in both wavelengths, implying that the vacuum pressure has an effect on the optical limiting properties of the graphene dispersions over a broad wavelength range from the visible to the near infrared.

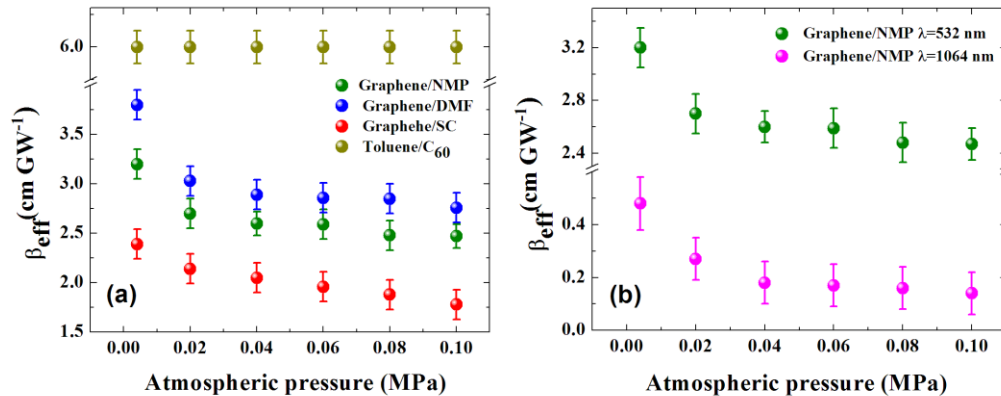


Fig. 5. The nonlinear extinction coefficient as a function of atmospheric pressure (a) for the graphene dispersions prepared in DMF (blue), NMP (green), SC (red) dispersions and C₆₀ (brown) in toluene at 532 nm, and (b) the NMP dispersions for 532 nm and 1064 nm.

Following the Beer-Lambert law, we can express the linear transmission of the graphene dispersions in the form of

$$T_0 = \exp(-\delta_0 NL) \quad (2)$$

where δ_0 is the linear extinction cross section. Since the decrease of the transmission is originated mainly from Mie scattering, the decreased transmission can also be written in the Beer–Lambert form of

$$T_{NL} = \exp(-\delta_{NL} NL) \quad (3)$$

where δ_{NL} is the nonlinear extinction cross section. Merging Eqs. (2) and (3) gives the ratio of the linear and nonlinear extinction cross sections

$$\delta_{NL} / \delta_0 = \ln T_{NL} / \ln T_0 \quad (4)$$

where we assume the number density of graphene nano-flakes N keeps constant in both the linear and the nonlinear regions. Figure 6(a) shows the normalized transmission and δ_{NL}/δ_0 as functions of incident intensity for a graphene dispersion with the transmission of 51%. Under the irradiation at 532 nm, the extinction cross section at 0.5 GW/cm² is ~2 times larger than the linear cross section at <0.02 GW/cm². For pulses at 1064 nm at 6 GW/cm², δ_{NL}/δ_0 at 0.1 MPa is ~1.6, which is improved to ~2.5 at 0.004 MPa. According to the theoretical simulation [29], the scattering cross section increases significantly with the increasing size of micro-bubbles, meanwhile the absorption cross section decreases until it is negligible when the bubbles grow, effectively limiting the incident power. Therefore, we consider the micro-bubbles as non-absorbing dielectric spheres and the corresponding scattering cross section can be expressed by Mie theory as [30]

$$\delta = \frac{2\pi r^2}{q^2} \sum_{l=1}^{\infty} (2l+1)(|a_l|^2 + |b_l|^2) \quad (5)$$

where a_l and b_l are the coefficients defined with Bessel function and its differentiation, l is an integer, q is the corresponding size parameter, r is the radius of the micro-scatters. Substituting Eq. (5) into Eq. (3) allows one to estimate T_{NL} as a function of the radius of micro-bubbles. The simulation results are depicted in Fig. 6(b) by assuming different densities of graphene nano-flakes in dispersions. As the increasing of the graphene number density, the bubble sizes required to extinct effectively the laser beam become smaller.

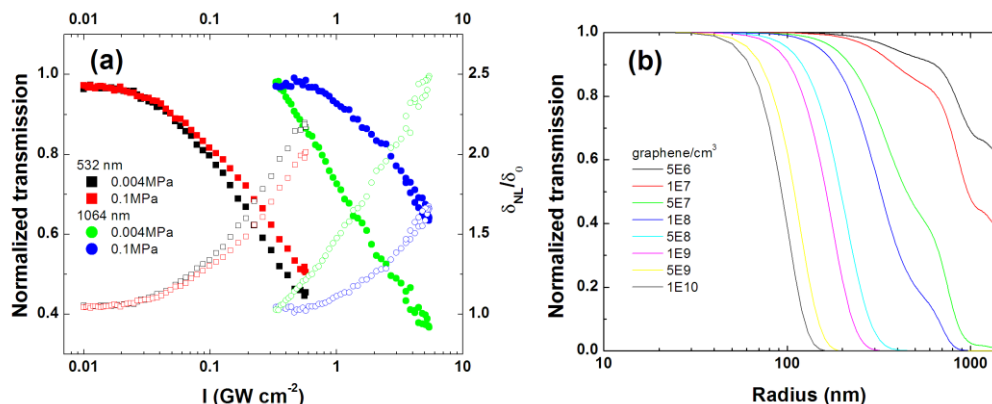


Fig. 6. (a) Normalized transmission (closed) and δ_{NL}/δ_0 (open) as functions of incident intensity for the graphene dispersions with the transmission of 51%. (b) Normalized transmission as a function of the radius of micro-bubbles.

4. Summary

In summary, we have successfully demonstrated by a modified Z-scan method that the vacuum pressure has controllable effect on the broadband NLO as well as optical limiting response for the graphene dispersions. Our results further confirm that the origin of optical limiting of the graphene dispersions is the solvent and/or carbon vapor bubble induced NLS, which can be tuned by the vacuum pressure. The nonlinear extinction coefficients of the graphene dispersions increased gradually with the reduction of the pressure for ns pulses at both 532 nm and 1064 nm. At the same linear transmission, the DMF dispersions showed a larger nonlinear extinction and superior optical limiting effects in comparison with the NMP and SC dispersions under the same vacuum pressure.

Acknowledgments

J.W. thanks the financial supports from the 100-Talent Program of Chinese Academy of Sciences, the National Natural Science Foundation of China (NSFC, No. 61178007), and Science and Technology Commission of Shanghai Municipality (STCSM Nano Project, No. 11nm0502400, Shanghai Pujiang Program 12PJ1409400). N.N.D. thanks the financial support from the China Postdoctoral Science Foundation (2012M520049). L.Z. thanks the financial supports from NSFC (No. 51072207), STCSM Excellent Academic Leader of Shanghai (No. 10XD1404600). W.J.B. gratefully acknowledges a visiting professorship for international scientists from the Chinese Academy of Sciences. His contribution towards this publication has also emanated from research supported in part by a research grant from Science Foundation Ireland (SFI) under Grant Number 12/IA/1306. S.F.Z. thanks STCSM and the Shanghai Natural Science Foundation (No. 12ZR1451800).